atmosphere

MDPI

Article

Cold Waves in East China and Their Response to Two Types of Arctic Amplification

Wei Tao [1,*], Yuman Ni [1] and Chuhan Lu [2]

[1] Anhui Meteorological Observatory, Hefei 230031, China; ni_yuman@163.com
[2] Key Laboratory of Meteorological Disaster, Ministry of Education/Collaborative Innovation Center on Forecast and Evaluation of Meteorological Disasters, Nanjing University of Information Science and Technology, Nanjing 210044, China; luchuhan@nuist.edu.cn
* Correspondence: taoweijanet@163.com

Received: 30 April 2020; Accepted: 27 May 2020; Published: 9 June 2020

Abstract: Cold waves occur frequently in East China, with their cold air source in the Arctic. Changes in the Arctic are often linked with Arctic amplification. The circulation anomaly associated with Arctic amplification is often represented by Arctic Oscillation (AO). In recent years, storms have frequently invaded the central Arctic region, resulting in dramatic changes in Arctic environment. In this paper, based on correlation studies, composite analysis, and case studies, the remote effects of the old and storm-induced Arctic amplification are compared, especially with regard to their impact on cold waves in East China. The results show that the AO can shed light on the interannual variation of cold events intermittently, although it cannot explain the increasing trend of cold waves in the southern part of East China. However, this long-term trend correlates well with storm activity. Cyclones are becoming more active in the western Arctic and anticyclones are intensifying in the eastern Arctic. In this scenario, the storm-induced warm advection could enhance the ridge over northeast Eurasia, the Siberian High expands southeastward, and cold air accumulates in northeast Asia, which cools the northern part of East China directly. The circulation around the Siberian High leads to a northeast wind in the southern part of East China, which plays a vital role in snowstorms. This study could improve our understanding of the global effects of Arctic changes and could enhance the prediction skill of cold waves.

Keywords: cold wave; Arctic oscillation; Arctic storm

1. Introduction

In this century, more frequent cold extremes are observed at midlatitudes [1]. For example, bitterly cold waves occurred in Europe and the USA during the winters of 2010/2011, 2013/2014, and 2014/2015 [2,3]. East Asia has also been repeatedly affected by cold waves in recent decades, with examples including the freezing disaster in southern China in early January 2008, January–February 2012, and the winter of 2015/2016 [4–6]. All the above cold events resulted in a huge amount of damage and great economic loss. Therefore, researchers have started to focus on midlatitude cold waves and their possible contributory factors. Given that most midlatitude cold waves originate from the the Arctic, we are motivated to explore the linkage between the Arctic changes and the midlatitude cold waves.

Temperatures have increased about twice as fast in the Arctic as in midlatitudes, which is known as Arctic amplification. Disparate mechanisms are responsible for the Arctic amplification, including sea ice, snow, cloud, solar cyclic, and the Planck and lapse rate effects [7–9]. Some studies have proposed that upward heat flux from an ice-free ocean warms the Arctic [10] and hence the prior-autumn Arctic sea ice exerts cross-seasonal influences on subsequent-winter circulations, which induce

stationary Rossby wave train propagation [11], the impact of which on the occurrence of East Asian snowstorms [12,13] leads to cooling of midlatitudes [14–17]. However, the influence of sea ice is still under discussion [6,9,18,19]. Because there has been an enormous reduction in Barents–Kara Sea ice since 2007, it should have been cold every winter, which has not been the case [19]. Francis [9] has suggested that sea ice is not the Arctic amplification; some other factors, such as water vapor, clouds, and stratosphere, which could change the atmospheric radiation and circulation, must be considered. Goosse [18] has suggested that the stable stratification conditions result in a larger lapse rate in high latitude than the tropic area, leading to a smaller increase of outgoing long-wave radiation, and thus accelerate Arctic amplification. However, Planck effects indicate that higher temperature increases longwave radiation which impedes Arctic warming. Ma and Zhu [6] pointed out that the extreme cold wave in January 2016 originated largely from natural internal atmospheric variability and was only modulated by the retreat of sea ice.

In early works, the natural internal atmospheric variability over high latitudes has been described in terms of the Northern Annular Mode (NAM) and the Arctic Oscillation (AO). NAM could represent the geopotential height anomaly from the stratosphere polar vortex to the surface [7]. AO is known as the near surface signature of NAM, which is believed to have important contemporaneous and cross-seasonal influences on East Asian weather and climate in some studies [20–24]. The negative phase of the AO is equivalent to a weak jet stream [25]. Such a condition is accompanied by persistent large meanders, which allow cold air to spread southward [26]. However, in the case of negative AO, it is not specified where the southward meander travels [19], and it does not necessarily cause the blocking events [27]. Therefore, some researchers suggests that AO should not be employed as a prototype for Arctic amplification [27,28], and some new circulation regimes have been proposed. An example is the Arctic rapid change phase (ARP), for which negative indicates the intensification and northward expansion of the Siberian High and the Aleutian Low [28]. Research has shown that the increased occurrence probability of strong Siberian High and associated Ural Ridge could lead to more frequent Eurasian blockings and could provide a circulation anomaly that favors severe extreme cold events in Eurasia [1,15,16,29,30]. However, there is a debate about the cause of blocking events. Some researchers have proposed that the reduction of the meridional temperature gradient would increase blocking events and amplitude [31], while some model studies have provided opposite results [32,33].

Cohen [8] have summarized some possible mechanisms linking Arctic change and midlatitude weather, including increasing the geopotential thickness over the Arctic, weakening of the thermal wind, stratosphere-troposphere coupling, stationary Rossby waves, and strengthening of the Siberian High and Aleutian Low. It has also pointed out that, rather than the local Arctic change (e.g., sea ice), the remote processes, such as heat and moisture transport from midlatitude to Arctic, also play an important role. In recent years, storm activities have exhibited greater fluctuations in the Arctic region [34–36]. Storm tracks and the associated atmospheric circulation have enhanced poleward heat and moisture transport into the Arctic Ocean and thus play a major role in Arctic amplification, owing not only to the warm advection but also to the moisture-induced increases in cloudiness and downward long-wave radiation [37]. Such heating effects and the circulation around the storm interact with sea ice and deform the Ural Ridge and Siberian High [19] and therefore can have an impact on cold waves in Eurasia. However, there is a lack of climatological statistics about the remote impact of Arctic storms, and it remains unclear how Arctic storms work with the typical Arctic circulation indices to alter downstream synoptic events.

In this study, based on 40 years of observational records, we compare the remote impacts of the AO and Arctic storm activity on cold waves and explore the underlying physical processes. Most previous research has focused on the impact of the Arctic on mid–high latitudes (40–70° N), but to the south of 40° N, Arctic-originated waves can interact with subtropical originated system to induce cold events, and this is still not thoroughly understood. The present study takes East China as an example, investigates the long-term variation of cold waves in its northern and southern parts separately, and analyzes their relationships with the AO and Arctic storms. In Section 2, we introduce the index used

in this paper to quantify Arctic circulation and cold wave activities. We then analyze the long-term changes and interannual variability of cold waves in the northern and southern parts of East China. The relationship between the AO, Arctic storms, and cold waves in East China will be explored in Section 3. Finally, in Section 4, we summarize the physical mechanisms underlying the linkage between the Arctic and cold waves in terms of a conceptual model.

2. Data and Methods

2.1. Criteria for a Cold Wave

According to the Chinese National Standard for Cold Waves, a cold wave event is considered to occur when either of the following conditions is met:

1. The daily minimum temperature decreases by 8 K in one day or by 10 K in two days, and the minimum temperature is lower than 277.15 K.
2. The daily mean temperature decreases by 8 K in one day or 10 K in two days, and the minimum temperature is lower than 277.15 K.

The daily minimum and mean temperatures are obtained by the 414 insu surface stations in East China, provided by the National Meteorological Information Center [38]. The cold waves during the winter monsoon season (from October to the following March) over the period 1979–2018 are analyzed in this study.

2.2. Arctic Circulation Index

The AO is a large-scale mode, characterized by winds circulating counterclockwise around the Arctic at around 60° N latitude. When the AO is in its positive phase, a ring of strong winds circulating around the North Pole acts to confine cold air across polar regions. In contrast, in the negative AO, this belt of wind becomes weaker and more distorted, which allows easier southward penetration of colder air. The AO index is constructed by projecting the 1000-mb height anomalies poleward of 20° N onto the loading pattern of the AO, which is defined as the leading mode of an empirical orthogonal function (EOF) analysis of monthly mean 1000 mb height during the period 1979–2000. In this study, the monthly mean AO indices during 1979–2018 are employed, which are taken from NCEP [39].

For Arctic storms, the storm identification and tracking algorithm developed by Zhang [34] is employed in this study based on the sea level pressure (SLP) from the NCEP 6-hourly reanalysis data. Storms to the north of 60° N with lifetime longer than 1 day are considered in this study. To quantify storm activity, we employed the cyclone activity index (CAI), which is the sum over all cyclone centers at a 6-hourly resolution of the differences between the cyclone central SLP and the climatological monthly mean SLP at corresponding grid points. It is an integrative index, including the number, duration, and intensity of storms. To investigate the impact of storm location, we calculated the CAI in the western and eastern hemispheres separately. If the storm center situates within 0–180° W, it is considered a west Arctic storm; otherwise, it is considered an east Arctic storm. The different CAIs between the east and west Arctic storms are described by an index: DET_CAI. A positive DET_CAI value implies that storms are active in the east hemisphere and calm in the west hemisphere and vice versa for a negative value.

3. Results

3.1. Climatology Background of East China

To better understand cold wave activities, the wintertime temperature climatology over East China is described here. With latitudes spanning from 20° N to 55° N, the temperature shows distinct features within this study region. In operational work, East China is roughly divided into two parts, southern and northern, along the boundary of the Qinling Mountains and the Huaihe River line,

as shown by the purple line in Figure 1. In the northern part, the monthly mean 2 m temperature is close to or lower than the freezing point, while it is generally above 273.15 K in the southern part (Figure 2).

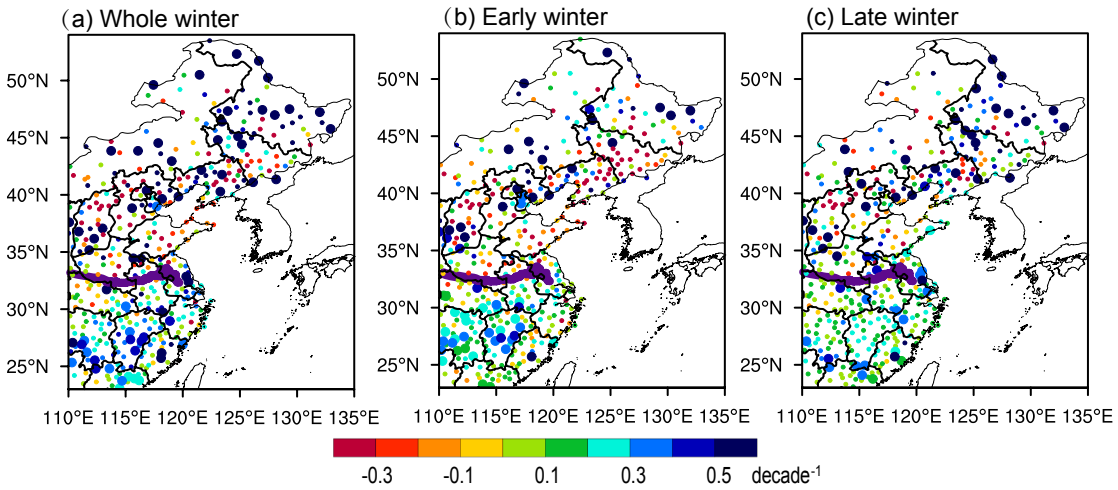

Figure 1. Trends of cold wave record numbers at each station in East China: The larger dots are the stations with a cold wave trend passing the 95% confidence level. The purple line is the Qinling Mountain–Huaihe River boundary, which forms the division between the northern and southern parts.

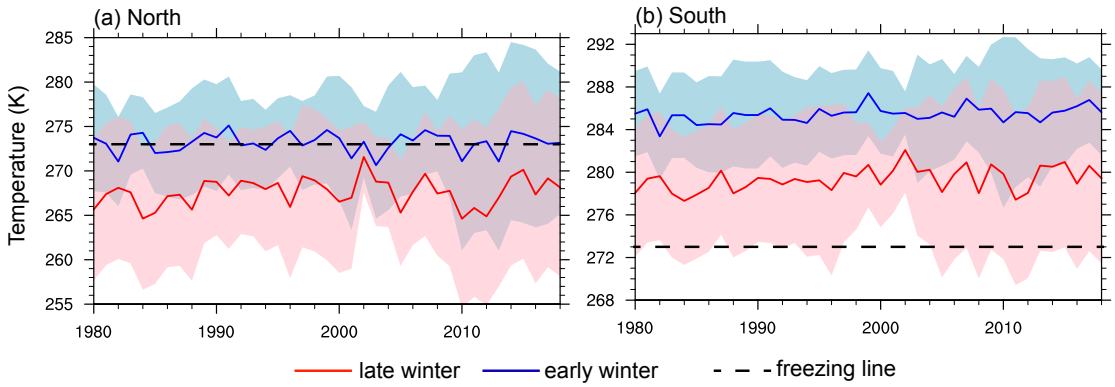

Figure 2. Time series of the areal mean temperatures in (**a**) the northern and (**b**) the southern parts of East China: The solid lines are the sub-seasonal mean temperatures, the shaded areas represent one standard deviation for the given sub-season (blue for early winter and pink for late winter; the gray color is the overlap of early and late winter), and the dashed lines represent 273.15 K.

The temperature also exhibits sub-seasonal differences. We divide the winter monsoon season into early winter (October–December) and late winter (January–March). As shown in Figure 2, the temperature exhibits opposite interannual variations in some years (e.g., 1980–1985 and 1996–2000, whereas temperatures in 1982 and 1997 were lower than the adjacent years in early winter and warmer in late winter) and supports the necessity to analyze early and late winter separately. In addition, in early winter, the mean temperature in the northern part is around 273.15 K, and it is far above the freezing line in the southern part. In late winter, although the monthly mean temperature in the southern part is above 273.15 K, its one standard deviation (calculated from the daily mean temperature) can fall below the freezing line. The freezing line is important because it could determine the phase of precipitation, which might further impact the surface albedo and radiation balance. That would mean snow being dominant over the northern part, since the temperature is around or lower than 273.15 K, while precipitation is usually in liquid phase over the southern part during early winter, and it could transform into snow if a cold wave happens in late winter. As the snow accumulated

on the ground, its high albedo would prevent the surface from storing heat from solar radiation and thus would intensify the cooling effect of the cold wave. Therefore, the mechanisms of induction of cold events are distinct in the northern and southern parts, and in early and late winter, which will be discussed in Sections 3.3 and 4. Furthermore, the AO shows a positive phase in early winter and a negative phase in late winter in some years (Figure S1 in the Supplementary Materials); Rinke [36] also suggested that more extreme cyclones happen in early winter. If we combined early and late winter together, these signals would be smoothed out.

3.2. Cold Waves in East China

The long-term change in cold waves is expressed by the trend of the cold wave record number of each station in Figure 1. From the viewpoint of the whole winter season, the frequency of cold wave activities tends to increase in some stations during 1979–2018. In the southern part, most stations show an increasing trend of cold wave record numbers at a rate of 0.2–0.4 decade^{-1}. This enhancement is more common in early winter. In the northern part, the long-term trend varies among stations. The frequency of cold waves increases at some stations and decreases at some others. Though there are a few stations present a significant increasing trend passing the 95% confidence level, around a 30% stations' trend could pass the 90% significance level. The different results of the significant tests could be explained by the large interannual variability of the cold wave activities.

To present the overall cold wave activities, we analyze the total record number, which is calculated as the sum of cold wave record numbers of all the stations in northern and southern East China (Figure 3). Since intense cold bursts are usually accompanied by strong winds, their impact can be widespread, which indicates that more stations experience the cold waves. Therefore, the total record number is an integrated index, which includes not only the cold wave number but also the intensity of cold waves in each winter. As shown in Figure 3, in the northern part, cold waves are usually active during early winter, while the southern part experiences more cold waves in late winter. There is a significant positive trend in the southern part during early winter, with a rate of increase of around 1.5 records per year. An increasing trend can also be identified in late winter, but this is contaminated by the large interannual variation and it does not pass the 95% confidence level. In the northern part, the evolution of the cold wave record number is dominated by the interannual variation, with little long-term trend.

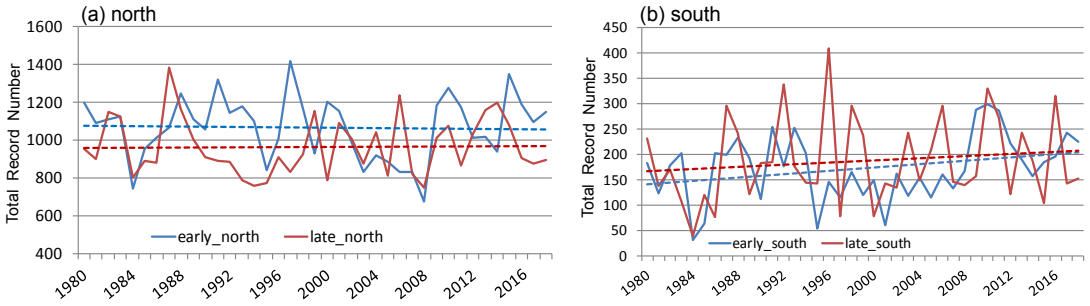

Figure 3. Interannual variation of total cold wave record numbers in (**a**) the northern and (**b**) the southern parts of East China during 1979–2018: The dashed lines show the 40-year trends.

3.3. The Impact of Arctic Amplification

In this study, the Arctic amplification is quantified by two Arctic circulation indices: AO and DET_CAI. First, an overview of the remote impact of the Arctic is obtained by comparing the normalized time series of cold wave record numbers, AO, and DET_CAI in Figure 4. In early winter, AO shows an opposite phase to the cold wave record number in the northern part in a few years (e.g., the early 1980s and 1996–1998), but the small correlation coefficient (−0.08) implies weak connection. In addition, the trend of AO is insignificant, while the cold wave record number in the southern

part increased during 1979–2018. However, such a long-term change in the southern East China cold waves could be explained partly by the negative trend of DET_CAI. There are more positive values of DET_CAI in the 1980s and more negative values after 2010. Such a scenario is consistent with the formation of the ARP [28] and is supported by a series of Atlantic storms intruding into the western Arctic [35] and the intensification of the Siberian High [40]. Furthermore, DET_CAI and southern cold waves show opposite interannual variations along with their opposite long-term trend, and their correlation coefficient reaches −0.35, passing the 95% confidence level. In late winter, the long-term trends of AO, DET_CAI, and cold waves are all insignificant. Dominated by interannual variation, the correlation coefficient between AO and cold waves is −0.32 in the north and −0.21 in the south, and that between DET_CAI and cold waves is −0.28 in the north and −0.26 in the south, all of them passing the 95% confidence level.

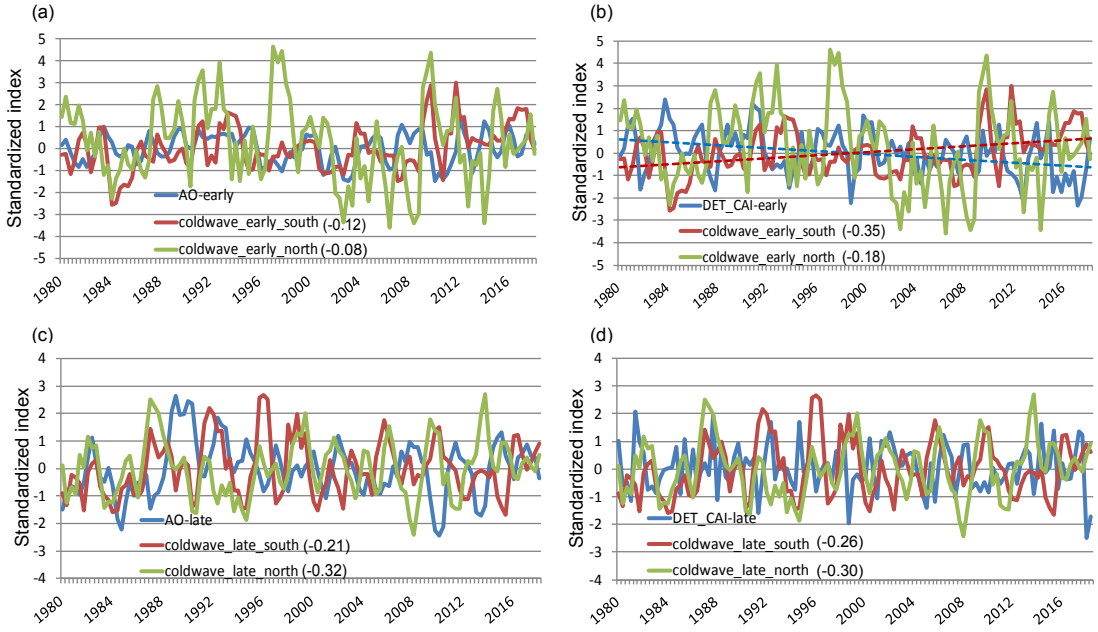

Figure 4. Standardized time series in early winter for all months during 1979–2018 of (**a**) the monthly Arctic Oscillation (AO) index and total cold wave record number and (**b**) the DET_CAI index and (**c**,**d**) that for late winter, respectively: The numbers in the legend indicate the correlation efficient with AO or DET_CAI. The dashed lines are the trend of DET_CAI and early winter cold wave number.

To investigate the underlying mechanisms of the correlation between Arctic circulation index and cold waves, we conduct composite analyses of circulations in months with pronounced positive and negative phases of the AO and DET_CAI indices. The threshold for pronounced AO and DET_CAI is ±1 standard deviation in the normalized index time series in Figure 4. The selected months are listed in Table 1. The variables investigated in these composite analyses include the sea level pressure (SLP), the wind field at 850 hPa, the temperature at 2 m and 850 hPa, and the geopotential heights at 500 hPa and 100 hPa. Their differences between the negative and positive phases are shown in Figure 5. It worth to notice that DET_CAI is an integrated index; the relevant composite differences are made up of both intensity and frequency of Arctic storms and Eurasia high systems.

During the early winter, the Arctic region is covered by an anticyclonic anomaly when the AO is in a negative phase (Figure 5a). The cold air over the Arctic is mainly transported to the Ural region by the northeast wind. The temperature advection in East Asia is weak (Figure 5b), and therefore, cold waves are unlikely to intensify. At the upper level (500–100 hPa), the anticyclone anomaly dominates the Arctic Ocean (Figure 5c), and the polar vortex (as shown by the 100 hPa geopotential height) becomes zonally orientated and shifted southward. On the south side of the polar vortex, a west wind

blows from the Black and Caspian Seas to Northeast China and the southward spread of cold air is moderate. Circulation is featured by large meanders under the negative phase of DET_CAI. Storms invade the west Arctic from the Atlantic (Figure 5d). To the east of the storms, the southwest wind transports warm air to the Barents–Kara Sea (Figure 5e). The accumulation of warm air enhances a ridge from near the surface to 100 hPa along the Eurasian coast (Figure 5d,f). The anticyclonic flow around the ridge advects cold air to the Siberian area (Figure 5e). Distorted by the ridge, the polar vortex exhibits a dipole structure, with one center over Siberia and the other over the west Arctic Ocean, coupling with the storms. Meanwhile, a zonal trough at 500 hPa situates under the polar vortex above the eastern Siberian area. The coupling of the ridge, zonal trough, and polar vortex generates a blocking situation (Figure 5f) which cools the region 90–140° E 50–60° N (Figure 5e). The cold air in this region frequently intrudes southward, and when it confronts the southwest wind in the southern part of East China, precipitation occurrs. Owing to the warm advection from the south, long-wave radiation from clouds, and the latent heat released by precipitation, the temperature is quite warm before and during the raining night (if there is precipitation in the morning, it would be warm before the rain), but it falls rapidly during the next day as the cold north wind becomes dominant. Night-time radiative cooling under a clear sky also intensifies the cold burst.

Table 1. Selected Months for Composite Analysis.

Index Phase	Months
+AO-Early Winter	198310, 198812, 199012, 199411, 200612, 200810, 200111, 201112, 201311, 201511
−AO-Early Winter	198011, 198112, 199512, 199612, 200012, 200211, 200212, 200512, 200912, 201012, 201212
+DET_CAI-Early Winter	198011, 198311, 198512, 198910, 199011, 199710, 199911, 200912, 201212, 201411
−DET_CAI-Early Winter	198111, 198612, 199311, 199811, 200311, 200810, 201012, 201112, 201211, 201312, 201412, 201512, 201611
+AO-Late Winter	198301, 198901, 198902, 199002, 199003, 199202, 199301, 199403, 200202, 200703, 201102, 201503
−AO-Late Winter	198403, 198501, 198701, 198702, 200103, 200401, 201001, 201002, 201101
+DET_CAI-Late Winter	198103, 198503, 198801, 199203, 199501, 200003, 200202, 200603, 201403, 201503, 201703
−DET_CAI-Late Winter	198102, 198802, 199103, 199901, 200102, 200502, 200601, 200703, 201201, 201802

The selected months are presented by 6 digits. The first 4 digits present the year, and the last 2 digits present the month.

The difference between late and early winter lies in the deepened 500 hPa trough and associated cold anomaly at 850 hPa over northeast China (Figure S2 in the Supplementary Material). With negative AO, the Aleutian Low shifts westward and couples with the Arctic high anomaly to shape north winds over the northeast Asian continent (Figure 5g). These north winds transport cold air to northeast China and result in a cold anomaly reaching 4 K at 850 hPa centering over this region (Figure 5h). Meanwhile, the polar vortex and 500 hPa zonal trough over northeast Eurasia are stronger than in early winter and the 500 hPa ridge moves from the Black and Caspian Seas to the Ural Mountains, generating the Ural high. The pressure gradient between the Ural high and zonal trough drives a northwest flow to cool East China (Figure 5i). Under the negative phase of DET_CAI, besides upper level anomaly, intensified Siberian High and Aleutian Low is also significant (Figure S2). Storms occur mainly in the west Arctic and the northwest Pacific. A strong Siberian High dominates the high-latitude region of the Eurasian continent, even extending to Northeast China (Figure 5j). Above this region, a 500 hPa

zonal trough and polar vortex are also maintained (Figure 5l). Under such conditions, the low-level cold anomaly exceeds 6 K, with its center over Northeast China (Figure 5k). The southern part of East China is mainly affected by the northeast wind, which is shaped by the pressure gradient between the Siberian High and storms over the northwest Pacific (Figure 5j,k). The northeast flow not only indicates cold advection, which causes the temperature to drop to freezing, but also brings moisture from the ocean, which induces snow in East China. The high albedo of the snow surface further amplifies the temperature reduction through radiative cooling.

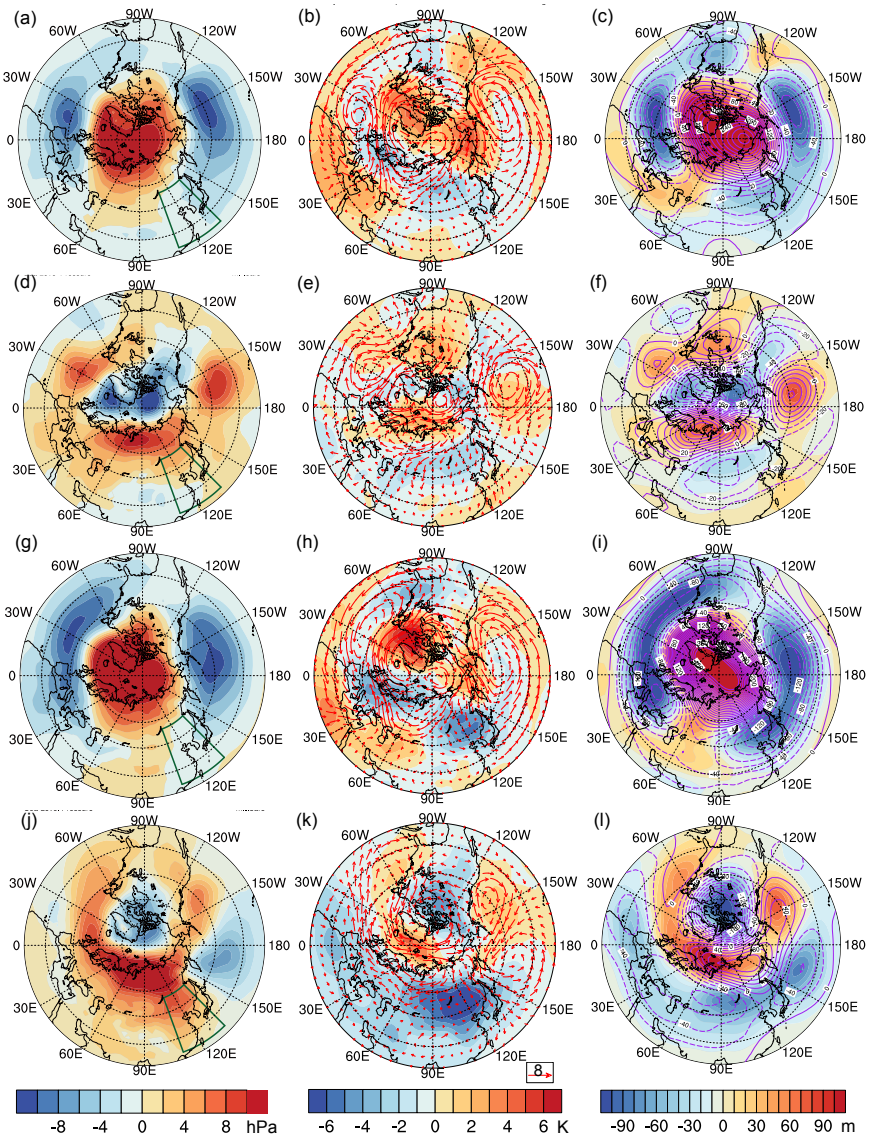

Figure 5. Composite differences between pronounced negative and positive AO in early-winter months in (**a**) sea level pressure (SLP), (**b**) in 2 m temperature and 850 hPa winds, and (**c**) in 500 hPa (filled color) and 100 hPa (contours) geopotential heights; (**d**–**f**) that for the difference between pronounced negative and positive DET_CAI in early-winter months, respectively; and (**g**–**l**) that for late-winter months, respectively.

The above analysis suggests that the invasion of west Arctic storms could contribute to the blocking events on the Eurasian north coast. To clarify this process, we conduct a lag-lead composite of 21 cases, for which the DET_CAI index is lower than −2 and persists for more than 2 days. The SLP, 850 hPa temperature advection, and 500 hPa geopotential height on the first day of the cases are compared with those of the next day (Figure 6). On day 1, a mild, high anomaly of the 500 hPa

geopotential height could be identified along the Eurasia north coast but its intensity was weaker than 120 m. Meanwhile, the storm centered over Greenland induces strong warm advection on its east side over the Scandinavia and Barents–Kara Sea. Such a warming effect enhances the geopotential height anomaly of this region to 150 m on day 2, and a strong Scandinavia ridge is built up. The well-matched location of the warm advection and the Scandinavia ridge indicate that the storm plays an important role in blocking. Under the influence of the Scandinavia ridge, the Siberia High expands northeastwards, and cold advection over the east Siberia suggests cold air accumulation, which favors the the cold waves in East China.

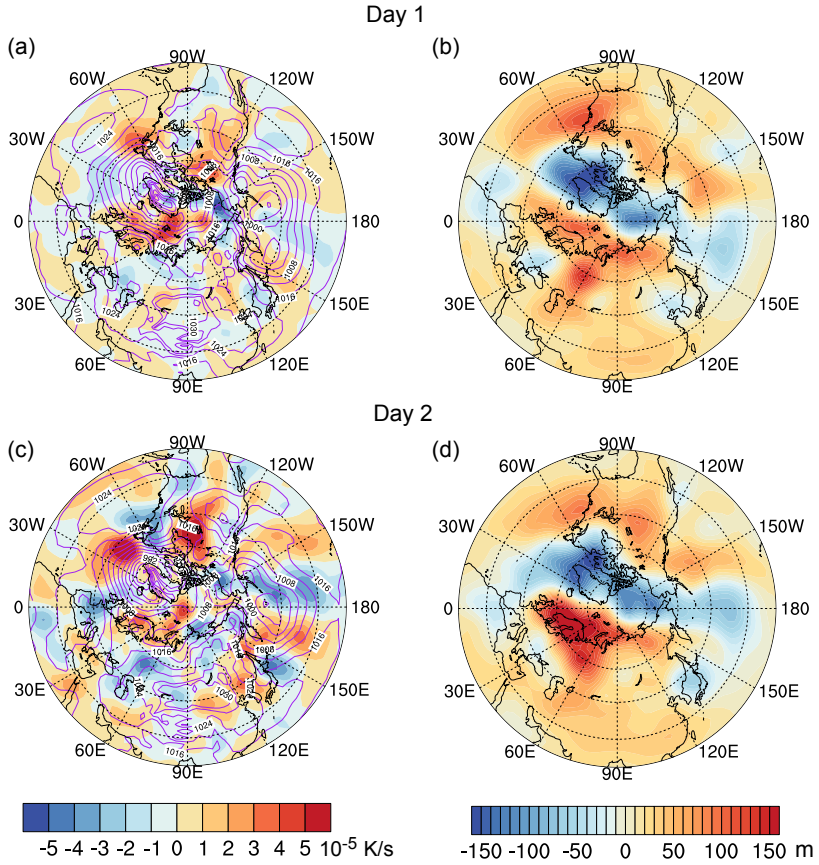

Figure 6. Composite (**a**) SLP (contours), 850 hPa temperature advection (filled color), and (**b**) 500 hPa geopotential height anomaly on large negative DET_CAI days and (**c**,**d**) that for fields on the next day, respectively.

To provide an insight into cold waves under the impact of DET_CAI and to give more synoptic clues to the operational forecast of cold waves, we conduct two case studies, one in early winter and the other in late winter. On 16 November 2017, northeast Asia was covered by a zonal trough at 500 hPa (Figure 7a). The Siberian High was around 1040 hPa, situated to the west of Lake Baikal (Figure 7c). The southwest wind dominated 25–40° N (Figure 7b), which brought water vapor (Figure 7c) and low clouds (Figure 7a) to the southern part of East China, and the associated warm advection increased the temperature to 288 K (Figure 7b). During 15–16 November, the heating induced by the warm advection was slightly larger than that caused by the precipitation released latent heat (Figure 7j). One day later, the zonal trough tended to become transverse to meridional (Figure 7d), indicating that the cold air had started to spread southward. The cold air confronted the warm south flow around 30–33° N (Figure 7e). Accompanied by rich water vapor (Figure 7f), the convergence generated pronounced precipitation. In addition to the blocking effects of the precipitable cloud (Figure 7d), the latent heat

of precipitation warmed up the air at the rate of around 0.3 K/h, which could overcome the cold advection (Figure 7j), so southern East China is still warm. On 18 November, a meridional trough was situated over northeast Asia. Behind the trough, the northwest flow led cold, dry air to East China. The rain stopped, and the cold advection achieved 0.6 K/h. Furthermore, with little cloud cover, radiative cooling also strengthened the cold break. As a result, the temperature fell by 10–14 K in 24 h.

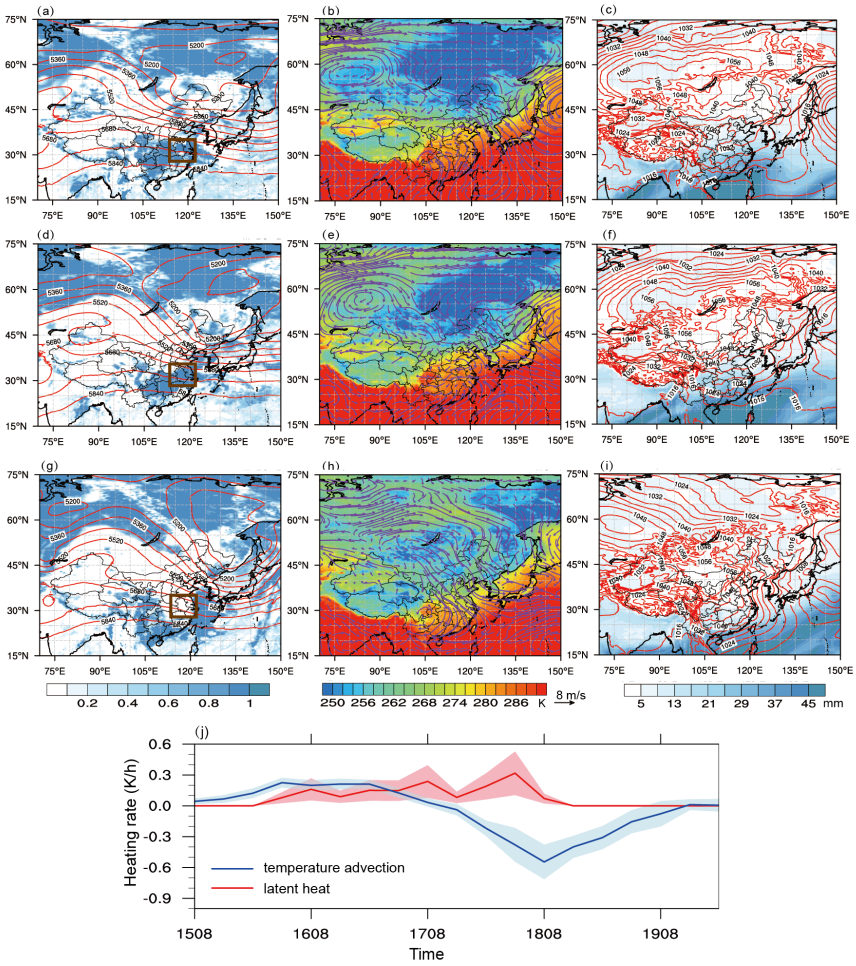

Figure 7. Synoptic analysis of a cold wave case in early winter: (**a**) Cloud cover and 500 hPa geopotential height, (**b**) 2 m temperature and 850 hPa winds, and (**c**) total precipitable water and SLP at 20 pm on 16 November 2017; (**d**–**f**) that at 20 pm on 17 November 2017, respectively; and (**g**–**i**) that at 20 pm on 18 November 2017, respectively. (**j**) The time-series of the mean heating rate caused by 850 hPa temperature advection and latent heat over the brown square in (**a**,**d**,**g**).The time coordinate is presented by 4 digits, with the first 2 digits indicating the date in November 2017 and the last 2 digits indicating the local time.

For the case of late winter of 2016, the 500 hPa vortex was embedded in a zonal trough with its center around 55° N on 21 January (Figure 8a). The Siberian High was much stronger than that in the early winter, exceeding 1056 hPa (Figure 8c). Covered by the thick snow accumulated during the early winter, the surface temperature of east Siberia was lower than 240 K, and this cold air was advected to Northeast China by the northwest wind (Figure 8b). Meanwhile, the temperature was around 276 K in southern China, which was warmed by the warm advection from the South China Sea (Figure 8b). At this time, the heating rate of warm advection and latent heat from weak precipitation was around 0.1 K/h (Figure 8j). One day later, the zonal trough was propagating southward, indicating that the cold air column was intruding into Northeast China (Figure 8d,e). Following the anticyclonic flow surrounding the Siberian High, the cold air was first blown to the Pacific and then turned back to

southern East China (Figure 8e,f). Since the temperature was around 273 K, and the easterly wind transported cold and humid air to East China around 30° N, snow occurred in this region. The snow enhanced the latent heating rate to 0.2 K/h (Figure 8j). On 23 January, snow stopped and a northerly wind dominated most of East China from the surface to 500 hPa, resulting in a maximum cold advection around 0.5 K/h (Figure 8g–j). In the daytime, the high albedo of the snow coverage prevented absorption of solar radiation, while in the nighttime, the clear sky allowed strong radiative cooling. All these processes intensified the cold event. The cooling effect of snow is further investigated by comparing the change of temperature over the surface with and without snow in this case. Snow depth of area B in Figure 9a was less than 1 cm, while most stations in area A were covered by snow with the depth of 1–20 cm. Located in the south, the temperature of area A was about 1 K higher than area B before the cold wave. With cold air outbreak during 22–23 January, the temperature dropped greatly in both areas but area A experienced a slightly larger decreasing rate. Once the cold air passed, temperature stopped decreasing in area B but it kept on dropping in area A. Because snow was accumulated over this area during 21–23 January, on 24 January, the high albedo of the snow prevented the surface from absorbing solar radiation. As a result, the mean temperature of area A is 2–3 K lower than that of area B (Figure 9b).

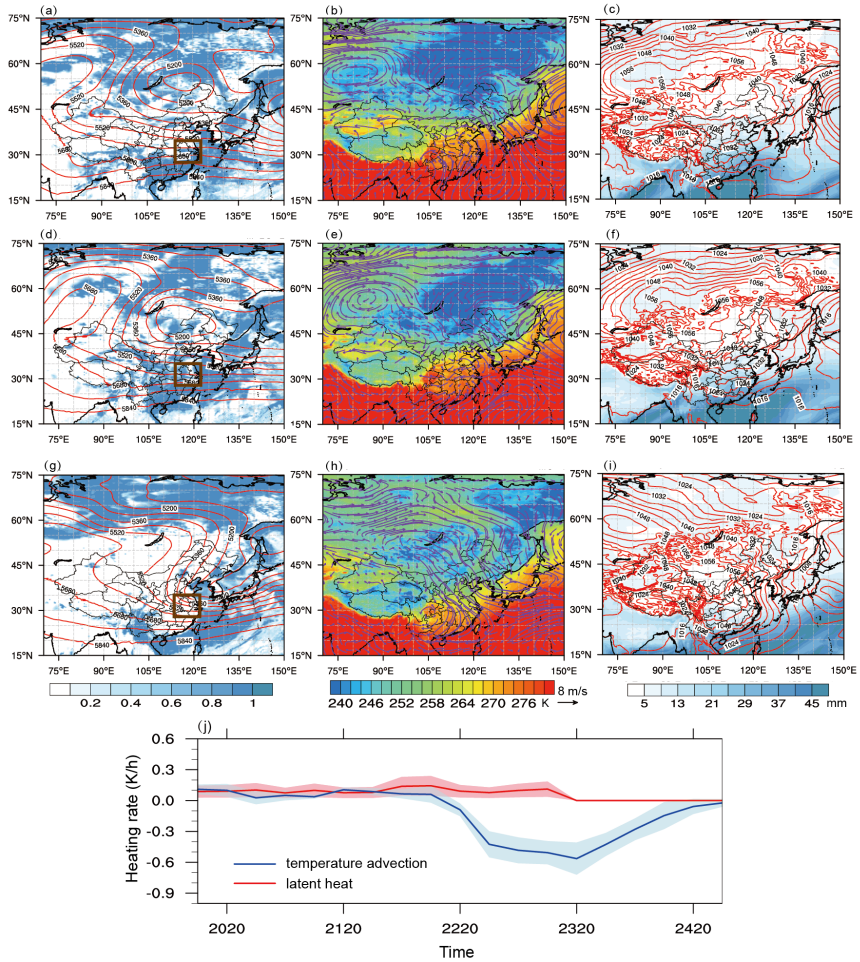

Figure 8. Synoptic analysis of a cold wave case in late winter: (**a**) Cloud cover and 500 hPa geopotential height, (**b**) 2 m temperature and 850 hPa winds, and (**c**) total precipitable water and SLP at 8 am on 21 January 2016; (**d**–**f**) that at 8 am on 22 January 2016, respectively; and (**g**–**i**) that at 2 am on 24 January 2016, respectively. (**j**) The time-series of the mean heating rate caused by 850 hPa temperature advection and latent heat over the brown square in (**a**,**d**,**g**).The time is presented by 4 digits, with the first 2 digits indicating the date in January 2016 and the last 2 digits indicating the local time.

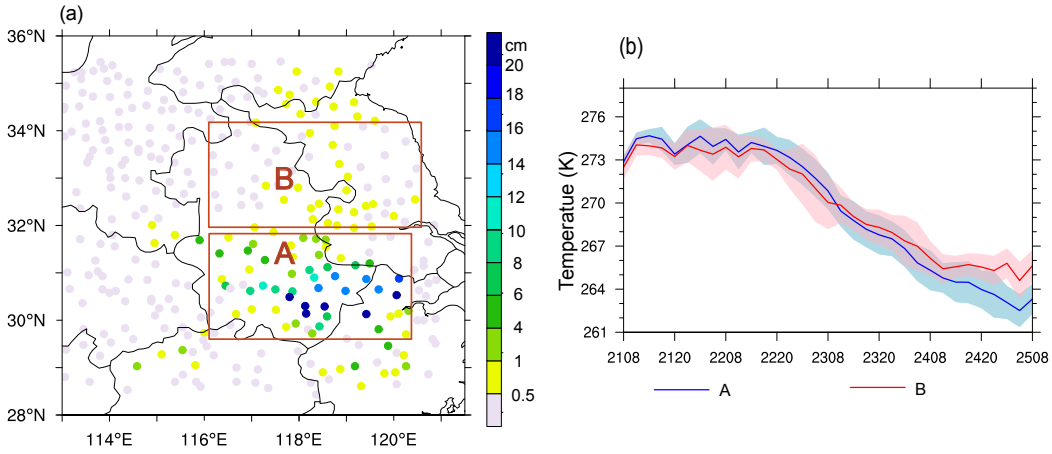

Figure 9. (**a**) The snow depth at 2 am on 24 January 2016 over the area surrounded by the brown rectangle in Figure 8g and (**b**) the time-series of the 2 m temperature during 21–25 January 2016 (the solid blue and red lines are the areal mean temperatures of areas A and B, and the shaded areas are their 1 standard deviation. The time coordinate is the same as that in Figure 8j).

4. Summary and Discussion

Under the background of climate change, the general circulation associated with Arctic amplification exhibits some new patterns. Previous studies have found that most of the Arctic warming interacted with the radiation balance adjustment induced by the retreat of sea ice. The change in temperature distribution modulated the circulation around the Arctic, which could be represented by the AO. This is a slow process and is considered as an old type of Arctic amplification in the present study. In recent years, storms have frequently invaded the Arctic region, leading to dramatic changes in wind, humidity, temperature, and sea ice. We have called this rapid process "storm-induced Arctic amplification". The impacts of the "storm-induced Arctic amplification" are affected by the locations of the storms, which have different remote impacts. If storms are in the western hemisphere, they may contribute to the blocking event, while storms could suppress the development of Siberia High if they are in the eastern hemisphere. The difference in storm activity between eastern and western Arctic regions are quantified by DET_CAI in this study.

AO and storm-induced Arctic amplifications have different impacts on cold waves in East China. The AO index can provide clues to the interannual variation of cold waves in late winter, and their correlation coefficient is -0.32 in northern China and -0.21 in southern China, passing the 95% confidence level. Such a relationship is consistent with the work of Chen [41], which suggests that the interannual variation of winter extreme cold days in the northern part of East China is closely linked to the AO. However, AO cannot explain long-term changes in cold wave activities. In early winter, cold waves in the southern part of East China have increased over the past 40 years, and their connection with AO is very weak. However, DET_CAI presents a decreasing trend in early winter during 1979–2018, which is negatively correlated with the cold waves in southern East China because anticyclones are enhanced in the eastern Arctic and a greater number of strong storms intrude into the western Arctic. In late winter, DET_CAI also shows a high negative correlation with cold waves in both northern and southern China. This scenario agrees with the results of previous research, which suggested that the Siberian High, Ural High, and strong Arctic storms contribute to cold waves [19,30,35].

The mechanisms by which the two types of Arctic amplification influence cold waves are summarized by the conceptual model in Figure 10. Under the negative phase of the AO, the Iceland Low and Aleutian Low are in the western hemisphere and are too far away to couple with the Siberian High to modulate circulation. The northeast wind steered by the Siberian High occurs at 50–60° N 90–120° E and thus has a small impact on East China. At the upper level, the atmosphere over the Arctic

Ocean is warm and cold air is moved to the northern Eurasian continent. In response, the polar vortex also shifts to the Eurasian region and westerly winds flow along the south edge of the polar vortex (Figure 10a). With a small meridional component and long-distance transport, the cold advection induced by the west wind is weak.

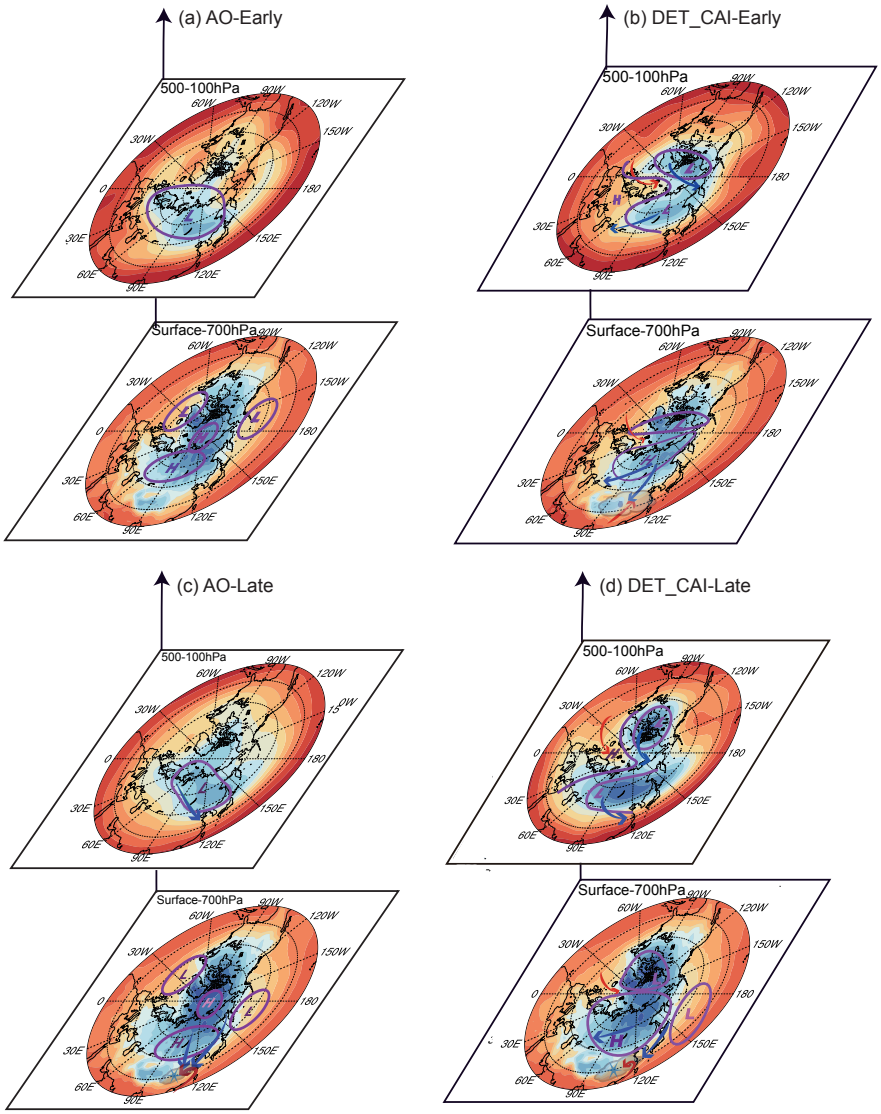

Figure 10. Conceptual model of the cold wave response to negative AO in (**a**) early and (**c**) late winter and (**b,d**) that for the response to negative DET_CAI, respective. The color shading represents the temperature, and the purple contours indicate the high and low systems. The red and blue arrows show warm and cold advections, respectively. The blue droplets indicate regions of rainfall, and the blue stars indicate regions of snow.

The basic difference between negative AO and negative DET_CAI is that a surface high system dominants the whole Arctic Ocean in the former scenario whereas storms occupy the west Arctic in the latter (Figure 10b). At the upper level, mid–high latitudes exhibit a stationary wave train pattern when DET_CAI is negative. Southerly winds on the eastern sides of the storms transport warm air from the Atlantic to the Barents–Kara Sea and thereby amplify the high ridge. In response, the polar vortex is split into a dipole structure, with one center over Siberia and the other over the west Arctic, coupling with the storms. The circulation around the high ridge and the polar vortex transports cold air from

the west Arctic to Siberia. The accumulation of cold air favors the intensification and expansion of the Siberian High. In the east of the Siberian High, a north wind blows over East Asia, which cools the northern part of East China directly. When this north wind meets the southwestern humid flow, precipitation occurs in the southern part of East China. At first, this region is warmed up by the warm advection and the latent heat of precipitation, but once the rain decays, the cold north wind becomes dominant and the temperature decreases dramatically.

Compared with early winter, the circulation of the negative AO in late winter is more conducive to cold waves. The polar vortex moves to northeast Asia and becomes more meridionally orientated. Following the circulation around the polar vortex, the northwest flow advects cold air from the Barents–Kara Sea to northern China. Meanwhile, the Aleutian Low moves to the eastern hemisphere and the Siberian High dominates northern China. The two systems shape the northeast flow, which acts as cold advection to southern China. This cold advection can drop the temperature to 273.15 K and can cause snow when it converges with warm south winds. For negative DET_CAI, the polar vortex and zonal trough are deeper than in early winter and the Siberian High exhibits broader coverage. The persistence of the polar vortex, zonal trough, warm ridge, and Siberian High provides a blocking structure, which benefits the outbreak of cold waves. In addition, storms are also active over the northwest Pacific, and coupling with the Siberian High, they contribute to the intensification of the northeast wind, in which the cold, moist air plays a key role in snowfall in southern China. After the snow has covered the land surface, its high albedo further reduces the temperature.

The importance of the Arctic amplification has been noticed in recent decades [23,31,42]. However, the mechanism of its formation and remote impacts, which vary with season and region, are worthy of further investigation. For example, what warms up the Arctic? Some studies have referred to the melting of sea-ice [17], while Hassanzadeh [27] has suggested that synoptic-eddy activities should be taken into consideration. This paper has revealed that Arctic storms could play an important role. The south wind on the east side of the storm transports warm air from the Atlantic Ocean to the Arctic, which warms up the Barents–Kara Sea greatly and thus intensifies the blocking along the Eurasia northwest coast and the Siberian High. The northern part of East China is directly affected by the Siberian High and by the accumulation of cold air in northeast Asia. The anticyclonic circulation around the Siberian High leads to an easterly wind in the southern part of East China, which plays a vital role in snowstorms in this region.

It worth to notice that negative DET_CAI could enhance the blocking events but not exactly equal to blocking. First, the blocking events is often evaluated by 500 hPa geopotential height while the DET_CAI is based on SLP. Since both DET_CAI and AO are based on SLP, DET_CAI could make up the surface circulation patterns which are missed in AO. Second, negative DET_CAI emphasizes the storms invading west Arctic and warm advections on their east side, which could warm up Arctic rapidly and intensify blocking (Figure 6). However, the blocking event alone could not explain the rapid temperature change near the Eurasian coast. Third, the storm could couple with the polar vortex, accompanied by the displacement of the polar vortex, and thus could contribute to the change of Arctic circulation [43].

The influence of cold waves on East China is very complicated owing to its location in the transition zone between midlatitudes and the subtropical region. This study has focused mainly on the impact of the Arctic. The interaction of Arctic storms, the East Asian monsoon, and subtropical wet flows will be explored in the future. The climatological relationships and the mechanisms revealed in this study can help improve understanding of the global effects of Arctic amplification and the prediction of cold waves.

Supplementary Materials: Supplementary Materials are available online at http://www.mdpi.com/2073-4433/11/6/612/s1.

Author Contributions: W.T. designed the research and wrote the first draft of the paper. W.T. and Y.N. analyzed the data. C.L. revised the first draft and provided useful insights. W.T., Y.N., and C.L. reviewed the manuscript. All authors have read and agreed to the published version of the manuscript.

Funding: This research is supported by the Natural Science Foundation of Anhui (No.1808085QD118) and the Key research and development project of Anhui (No.20190407020099).

Acknowledgments: The authors thank NCEP for producing reanalysis data. The computing resources were provided by the Arfctic Region super computing Center at the University of Alaska Fairbanks and the super computer in Anhui Meteorological Observatory.

Conflicts of Interest: The authors declare no conflict of interest.

References

1. Ma, S.; Zhu, B.C.; Liu, T.; Zhou, Y.; Ding, Y.; Orsolini, J. Polarized response of East Asian winter temperature extremes in the era of Arctic warming. *J. Clim.* **2018**, *31*, 5543–5557. [CrossRef]
2. Peterson, T.C.; Stott, P.A.; Herring, S. Explaining extreme events of 2011 from a climate perspective. *Bull. Am. Meteor. Soc.* **2012**, *93*, 1041–1067. [CrossRef]
3. Herring, S.C.; Hoell, A.; Hoerling, M.P.; Kossin, J.P.; Schreck, C.J., III; Stott, P.A. Explaining extreme events of 2015 from a climate perspective. *Bull. Am. Meteorol. Soc.* **2016**, *97*, S1–S145. [CrossRef]
4. Ding, Y.; Wang, Z.; Song, Y.; Zhang, J. The unprecedented freezing disaster in January 2008 in southern China and its possible association with the global warming. *Acta Meteorol. Sin.* **2008**, *22*, 538–558.
5. Gong, Z.; Feng, G.; Ren, F.; Li, J. A regional extreme low temperature event and its main atmospheric contributing factors. *Theor. Appl. Climatol.* **2014**, *117*, 195–206. [CrossRef]
6. Ma, S.; Zhu, C. Extreme cold wave over east asia in january 2016: a possible response to the larger internal atmospheric variability induced by Arctic warming. *J. Clim.* **2019**, *32*, 1203–1216. [CrossRef]
7. Roy, I. Solar cyclic variability can modulate winter Arctic climate. *Sci. Rep.* **2018**, *8*, 4864. [CrossRef] [PubMed]
8. Cohen, J.; Zhang, X.; Francis, J.; Jung, T.; Kwok, R.; Overland, J.; Ballinger, T.J.; Bhatt, U.S.; Chen, H.W.; Coumou, D.; et al. Divergent consensuses on Arctic amplification influence on midlatitude severe winter weather. *Nat. Clim. Chang.* **2020**, *10*, 20–29. [CrossRef]
9. Francis, J.A. Why Are Arctic Linkages to Extreme Weather Still up in the Air? *Bull. Am. Meteorol. Soc.* **2017**, *98*, 2551–2557. [CrossRef]
10. Petty, A.A. A possible link between winter Arctic sea ice decline and a collapse of the Beaufort High? *Geophys. Res. Lett.* **2018**, *45*, 2879–2882. [CrossRef]
11. Li, J.; Zheng, F.; Sun, C.; Feng, J.; Wang, J. Pathways of influence of the northern hemisphere mid-high latitudes on east asian climate: a review. *Adv. Atmos. Sci.* **2019**, *36*, 902–921. [CrossRef]
12. Wu, Z.W.; Li, J.P.; Jiang, Z.H.; He, J.H. Predictable climate dynamics of abnormal East Asian winter monsoon: Once-in-a-century snowstorms in 2007/2008 winter. *Clim. Dyn.* **2011**, *37*, 1661–1669. [CrossRef]
13. Screen, J.A.; Simmonds, I. Exploring links between Arctic amplification and mid-latitude weather. *Geophys. Res. Lett.* **2013**, *40*, 959–964. [CrossRef]
14. Cohen, J.; Screen, J.A.; Furtado, J.C.; Barlow, M.; Whittleston, D.; Coumou, D.; Francis, J.; Dethloff, K.; Entekhabi, D.; Overland, J.; et al. Recent Arctic amplification and extreme mid-latitude weather. *Nat. Geosci.* **2014**, *7*, 627–637. [CrossRef]
15. Mori, M.; Watanabe, M.; Shiogama, H.; Inoue, J.; Kimoto, M. Robust Arctic sea-ice infuence on the frequent Eurasian cold winters in past decades. *Nat. Geosci.* **2014**, *7*, 869–873. [CrossRef]
16. Honda, M.; Inoue, J.; Yamane, S. Infuence of low Arctic sea-ice minima on anomalously cold Eurasian winters. *Geophys. Res. Lett.* **2009**, *36*, L08707. [CrossRef]
17. Tang, Q.; Zhang, X.; Yang, X.; Francis, J.A. Cold winter extremes in northern continents linked to Arctic sea ice loss. *Environ. Res. Lett.* **2013**, *8*, 014036. [CrossRef]
18. Goosse, H.; Kay, J.E.; Armour, K.C.; Bodas-Salcedo, A.; Chepfer, H.; Docquier, D.; Jonko, A.; Kushner, P.J.; Lecomte, O.; Massonnet, F.; et al. Quantifying climate feedbacks in polar regions. *Nat. Commun.* **2018**, *9*, 1919. [CrossRef]
19. Tachibana, Y.; Komatsu, K.K.; Alexeev, V.A.; Cai, L.; Ando, Y. Warm hole in Pacific Arctic sea ice cover forced mid-latitude Northern Hemisphere cooling during winter 2017–2018. *Sci. Rep.* **2019**, *9*, 5567. [CrossRef]

20. Sun, C.; Li, J.P.; Zhao, S. Remote influence of Atlantic multidecadal variability on Siberian warm season precipitation. *Sci. Rep.* **2015**, *5*, 16853. [CrossRef]
21. Wu, Z.; Li, X.; Li, Y.; Li, Y. Potential influence of Arctic sea ice to the interannual variations of East Asian spring precipitation. *J. Clim.* **2016**, *29*, 2797–2813. [CrossRef]
22. Wu, J.J.; Wu, Z.W. Interdecadal change of the spring NAO impact on the summer Pamir-Tienshan snow cover. *Int. J. Climatol.* **2019**, *39*, 629–642. [CrossRef]
23. Overland, J.E.; Dethloff, K.; Francis, J.A.; Hall, R.J.; Hanna, E.; Kim, S.J.; Screen, J.A.; Shepherd, T.G.; Vihma, T. Nonlinear response of mid-latitude weather to the changing Arctic. *Nat. Clim. Chang.* **2016**, *6*, 992–999. [CrossRef]
24. Shepherd, T.G. Effects of a warming Arctic. *Science* **2016**, *353*, 989–990. [CrossRef]
25. Tompson, D.W.J.; Wallace, J.M. Regional climate impacts of the Northern Hemisphere annular mode. *Science* **2001**, *293*, 85–89. [CrossRef]
26. Nakamura, H.; Fukamachi, T. Evolution and dynamics of summertime blocking over the Far East and the associated surface Okhotsk high. *Q. J. R. Meteorol. Soc.* **2004**, *130*, 1213–1233. [CrossRef]
27. Hassanzadeh, P.; Kuang, Z. Blocking variability: Arctic Amplification versus Arctic Oscillation. *Geophys. Res. Lett.* **2015**, *42*, 8586–8595. [CrossRef]
28. Zhang, X.D.; Sorteberg, A.; Zhang, J.; Gerdes, R.; Comiso, J.C. Recent radical shifts of atmospheric circulations and rapid changes in Arctic climate system. *Geophys. Res. Lett.* **2008**, *35*, L22701. [CrossRef]
29. Kug, J.-S.; Jeong, J.-H.; Jang, Y.-S.; Kim, B.-M.; Folland, C.K.; Min,S.-K.; Son, S.-W. Two distinct influences of Arctic warming on cold winters over North America and East Asia. *Nat. Geosci.* **2015**, *8*, 759–762. [CrossRef]
30. Lu, C.; Xie, S.; Qin, Y.; Zhou, J. Recent Intensified Winter Coldness in the Mid-High Latitudes of Eurasia and Its Relationship with Daily Extreme Low Temperature Variability. *Adv. Meteorol.* **2016**, *2016*, 3679291, doi:10.1155/2016/3679291. [CrossRef]
31. Francis, J.A.; Vavrus, S.J. Evidence linking Arctic amplification to extreme weather in mid-latitudes. *Geophys. Res. Lett.* **2012**, *39*, L06801. [CrossRef]
32. Hassanzadeh, P.; Kuang, Z.; Farrell, B.F. Responses of midlatitude blocks and wave amplitude to changes in the meridional temperature gradient in an idealized dry GCM. *Geophys. Res. Lett.* **2014**, *41*, 5223–5232. [CrossRef]
33. Blackport, R.; Screen, J.A. Insignificant effect of Arctic amplification on the amplitude of midlatitude atmospheric waves. *Sci. Adv.* **2020**, *6*, eaay2880. [CrossRef] [PubMed]
34. Zhang, X.; Walsh, J.E.; Zhang, J.; Bhatt, U.S.; Ikeda, M. Climatology and interannual variability of Arctic cyclone activity: 1948–2002. *J. Clim.* **2004**, *17*, 2300–2317. doi:10.1175/1520-0442(2004)017<2300:CAIVOA>2.0.CO;2. [CrossRef]
35. Kim, B.M.; Hong, J.Y.; Jun, S.Y.; Zhang, X.; Kwon, H.; Kim, S.J.; Kim, J.H.; Kim, S.W.; Kim, H.K. Major cause of unprecedented Arctic warming in january 2016: critical role of an atlantic windstorm. *Sci. Rep.* **2017**, *7*, 40051. [CrossRef] [PubMed]
36. Rinke, A.; Maturilli, M.; Graham, R.M.; Matthes, H.; Handorf, D.; Cohen, L.; Hudson, S.R.; Moore, J.C. Extreme cyclone events in the Arctic: Wintertime variability and trends. *Environ. Res. Lett.* **2017**, *12*, 094006. [CrossRef]
37. Villamil-Otero, G.A.; Zhang, J.; He, J.; Zhang, X. Role of extratropical cyclones in the recently observed increase in poleward moisture transport into the Arctic ocean. *Adv. Atmos. Sci.* **2018**, *35*, 85–94. [CrossRef]
38. Daily Observation from NMIC. Available online: http://data.cma.cn/data/cdcdetail/dataCode/SURF_CLI_CHN_MUL_DAY_V3.0.html (accessed on 1 January 2020).
39. AO Index from NCEP. Available online: https://www.cpc.ncep.noaa.gov/products/precip/CWlink/daily_ao_index/ao_index.html (accessed on 1 January 2020).
40. Zhang, X.; Lu, C.; Guan, Z. Weakened cyclones, intensified anticyclones and recent extreme cold winter weather events in eurasia. *Environ. Res. Lett.* **2012**, *7*, 044044. [CrossRef]
41. Chen, S.F.; Chen, W.; Wei, K. Recent trends in winter temperature extremes in eastern China and their relationship with the Arctic Oscillation and ENSO. *Adv. Atmos. Sci.* **2013**, *30*, 1712–1724. [CrossRef]

42. Vihma, T. Effects of Arctic sea ice decline on weather and climate: A review. *Surv. Geophys.* **2014**, *35*, 1175–1214. [CrossRef]
43. Tao, W.; Zhang, J.; Fu, Y.; Zhang, X. Driving roles of tropospheric and tratospheric thermal anomalies in intensification and persistence of the Arctic Superstorm in 2012. *Geophys. Res. Lett.* **2017**, *44*, 10017–10025. [CrossRef]